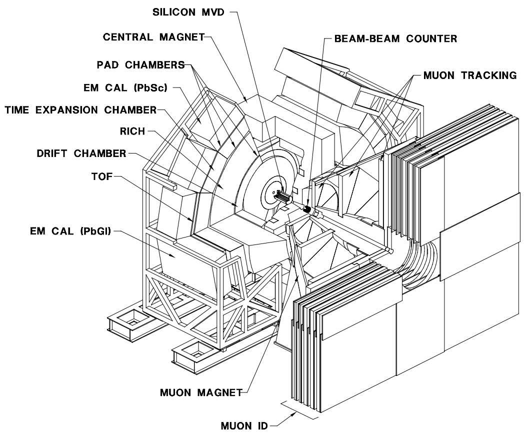

Figure 1. Schematic diagram of the PHENIX detector.

Particle Identification in TEC/TRD Prototypes for the PHENIX Detector at RHIC

B. Libby[a], A.Chikanian[b,†], S. Coe[b]
J. Dunlop[b], W. Guryn[c], J.C. Hill[a],
B. Johnson,[c], S. Kumar[b], Y. Makdisi[c],
J. Nagle[b],E. O'Brien[c], and N. Smirnov[b,‡]

[a]Iowa State University, Ames, IA
[b]Yale University, New Haven, CT
[c]Brookhaven National Laboratory, Upton, NY

1 Abstract

The tracking system in the PHENIX detector at RHIC has been designed to track charged particles in a high track density environment (dN_c/dy=1500). This corresponds to ~500 charged particles, primarily pions, in the fiducial volume of the detector, with a spectrum peaked at ~250 MeV/c. The TEC/TRD subsystem will track all charged particles and contribute to the particle identification between 200 MeV/c and 2.5 GeV/c by performing fine sampling energy loss (dE/dx) measurements. Prototype chambers were tested in a secondary beam of negatively charged particles at the AGS. An electron-pion separation at levels up to a factor of 200 by dE/dx was measured. This separation factor was measured as a function of the particle momentum and angle, and the gain and gas mixture used in the chamber.

2 INTRODUCTION

The PHENIX detector at RHIC, shown in Fig. 1, has been designed to measure physics signatures associated with the formation of the quark-gluon plasma in heavy ion collisions through the detection of photons, hadrons, and lepton pairs[1]. The Time Expansion Chamber (TEC) subsystem provides track vectors between the RICH and EmCal subsystems and contributes to the electron-pion discrimination of the entire detector by performing fine-sampling dE/dx measurements of charged particles passing through it.

As the charged particle passes through the TEC (Fig. 2), the electron clusters formed by the ionization of the gas drift toward the anode wires where charge amplification occurs. The signal from each anode wire is read out through a premplifier and shaping amplifier, and digitized with a Flash-ADC so that the time structure of the signal and the pulse height can

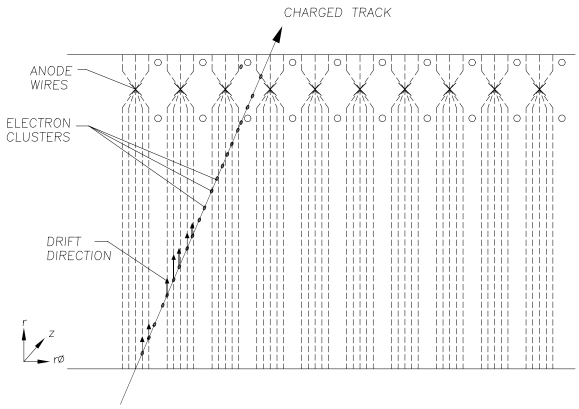

Figure 2. Schematic diagram showing the effect of a charged particle passing through a TEC. The drift distance is 30 mm, with 4 mm anode wire pitch and 3 mm between anode (dots) and cathode (circles)wire planes. The drift cathode plane is along the bottom of the figure.

be determined. This allows many independent measurements of the pulse height (or the dE/dx) in each individual FADC time bucket and also reconstruction of the track vector. In the momentum region of interest (200 MeV/c to 2.5 GeV/c), the average energy loss for electrons in each gas layer sampled by the FADC will be greater than that for pions, as described by the Bethe-Block formula. By making many independent measurements of the energy loss of charged particles in these chambers, the mean dE/dx for electrons and pions can be determined accurately and good particle species discrimination can be achieved.

In the baseline version of PHENIX, the TEC will consist of four planes of detector, giving a total of 12 cm of drift distance, and will be filled with P-10 gas. The system will be upgraded by the addition of two more planes of chambers, interleaving the planes with radiator foils, and using a Xe-based gas mixture for the detection of transition radiation. The subsystem will simultaneously perform its tracking, dE/dx, and transition radiation detection tasks.

3 THE TEST RUN

The four TECs used in the test run had active areas of 20×20 cm^2 with the anode-cathode configuration described in Fig. 2. The anode wires were read out through single channel hybrid preamplifiers and shaping amplifiers with a 70 ns shaping time and tail cancellation. After shaping, the signal was digitized by a 6 bit (2V full scale), 41 MHz FADC with a memory depth of 256 bins. The entire data acquisition system was controlled by a Motorola 68040 processor resident in a VME crate.

The test run took place in the B2 test beam of the AGS at BNL, using a secondary beam which consisted primarily of electrons and pions. A coincidence between three scintillation counters was used to define a minimum bias (MB) trigger, and two Cerenkov counters in coincidence with the MB trigger was used to define an electron. A hole veto counter was used in the offline data analysis, and a lead glass calorimeter was used offline to independently identify electrons and pions.

The TECs were tested under different conditions to evaluate their performance. Data was taken at a variety of fixed beam momenta which ranged between 0.5 and 2.5 GeV/c and incident angles from 0° to 20°. The chambers were operated at effective gas gains (not corrected for ballistic deficit) of 2500, 5000, and 10,000. The data was taken primarily with P-10 gas, but data was also taken with Xe-based gas mixtures to compare to previous results with different chambers.

4 dE/dx RESULTS

To evaluate the dE/dx performance of the chambers, tracks from single particles were selected. Tracks from separate particles, either electrons or pions, were combined to reach the equivalent of either 12 cm or 18 cm of drift distance. Once data had been accumulated for either electrons or pions, the mean energy loss for the event was determined through a truncated mean procedure that eliminated the high dE/dx values in the tails of the Landau distributions[2−5]. In this analysis, the highest 50% of the dE/dx values were eliminated. The truncated mean dE/dx distributions for both electrons and pions for a typical run with P-10 gas is shown in Fig. 3 for 12 cm (140 time samples) and 18 cm (210 time samples) drift distance. The distributions for 18 cm are narrower than those for 12 cm, and the overlaps between electrons and pions have decreased, due to the increased number of dE/dx measurements in the determination of the truncated mean. The truncated mean dE/dx distributions for electrons and pions for 12 cm (232 time samples) and 18 cm (348 time samples) of 95%-Xe-5%-C_4H_{10} are shown in Fig. 4. The distributions are narrower than those for 12 cm and 18 cm, respectively, of P-10, and the overlap even less, because the dE/dx per millimeter of gas is larger in the Xe mixture than in P-10. Additionally, the electron clusters have a lower drift velocity (longer drift time) in the Xe mixture than in P-10. Thus there are more independent dE/dx measurements for each track in the Xe mixture than in P-10.

A 90% cut in the electron efficiency is made, and the percentage of pions included in that cut is determined, giving the pion efficiency. The lower the pion efficiency, the higher the separation factor between electrons and pions. A plot

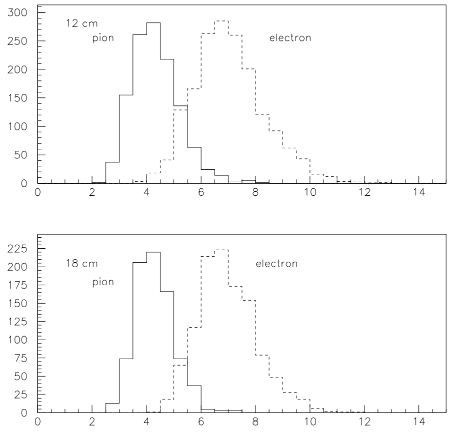

Figure 3. Truncated mean dE/dx distributions in FADC counts for electrons and pions for 12 cm (upper) and 18 cm (lower) of P-10 gasat 20° particle incident angle, 0.5 GeV/c, 5000 effective gain.

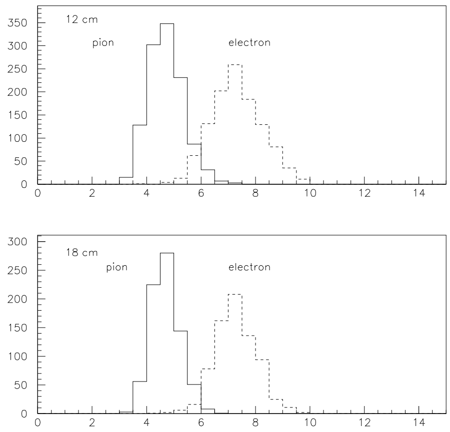

Figure 4. Truncated mean dE/dx distributions in FADC counts for electrons and pions for 12 cm (upper) and 18 cm (lower) of 95% Xe- 5%C_4H_{10} at 20° particle incident angle, 1.0 GeV/c, 5000 effective gain.

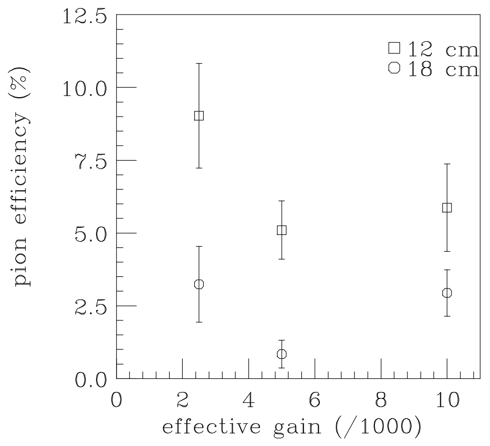

Figure 5. Pion efficiency as a function of effective gas gain in P-10 at 90% electron efficiency, 20° tracks.

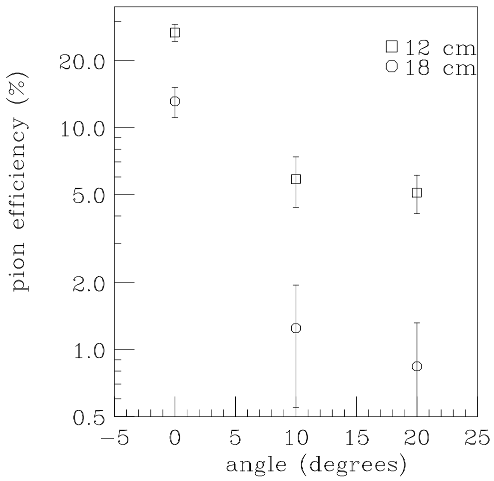

Figure 6. Pion efficiency as a function of particle incident angle in P-10 at 90% electron efficiency, 5000 effective gain at 0.5 GeV/c.

of pion efficiency as a function of effective gas gain for 20°, 0.5 GeV/c tracks in P-10 is shown in Fig. 5. The optimal effective gas gain is approximately 5000. All other P-10 data shown will be for runs at that gain.

The pion efficiency for 0.5 Gev/c particles P-10 and at various angles is shown in Fig. 6. The low separation between electrons and pions at 0° has been postulated as being due to space charge saturation at the anode wire. However, further investigation of this effect is required. The separation is constant between 10° and 20°, giving a factor of ~100 separation for 18 cm drift distance. Pion efficiencies for 20° tracks in both P-10 and 95% Xe as a function of momentum are shown in Fig. 7. The separation in P-10 worsens as momentum increases and the pions become more relativistic. The separation in the Xe mixture is higher, even at higher

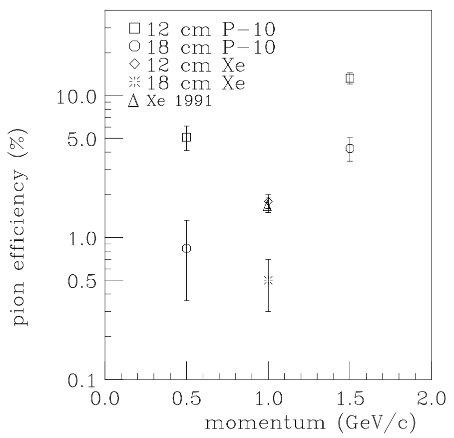

Figure 7. Pion efficiency as a function of momentum for 20° tracks at 90% electron efficiency for different gas mixtures.

momentum, than that in P-10 because of the greater energy loss per millimeter of gas in Xe. The experimentally separation factors were consistent with those determined from simulations of the detector performance[6]. Simultaneous dE/dx and transition radiation measurements[7] that was taken during this run is currently being analyzed.

5 SUMMARY

In tests of small prototype TEC's for the PHENIX detector, electron-pion separation factors of up to 200 were achieved. The optimal effective gas gain was determined to be close to 5000 in P-10 gas, and the angular dependence of the separation factor was characterized.

6 Acknowledgements

The authors would like to thank Carter Biggs and Dave Dayton for their technical assistance during the run. This work was supported by the United States Department of Energy.

† on leave from Lebedev Institute of Physics, Moscow, Russia
‡ on leave from PNPI, St. Petersburg, Russia

REFERENCES

1. PHENIX Conceptual Design Report, W.L. Kehoe, ed. (1993)
2. T. Ludlum, et al, IEEE Trans. Nucl. Sci. NS-28 (1981) 439.
3. A. Iminishi, et al, NIM 207 (1983) 357.
4. E. O'Brien, et al, IEEE Trans. Nucl. Sci. 40:2 (1993) 153.
5. E. O'Brien, et al, Nucl. Phys. A556 (1993) 615c.
6. N. Smirnov, private communication.
7. V. Bashkirov, et al, ATLAS Internal Note.